Journal of Controlled Release 350 (2022) 460–470

Contents lists available at ScienceDirect

Journal of Controlled Release

journal homepage: www.elsevier.com/locate/jconrel

IL-11Rα-targeted nanostrategy empowers chemotherapy of relapsed and patient-derived osteosarcoma

Jingjing Jiang [a,b,1], Renxian Wang [c,1], Liang Yang [a], Yongjie Sha [a], Songsong Zhao [a], Jianxun Guo [c], Dafu Chen [c,*], Zhiyuan Zhong [a,b,**], Fenghua Meng [a,**]

[a] Biomedical Polymers Laboratory, College of Chemistry, Chemical Engineering and Materials Science, and State Key Laboratory of Radiation Medicine and Protection, Soochow University, Suzhou 215123, PR China
[b] College of Pharmaceutical Sciences, Soochow University, Suzhou 215123, PR China
[c] Laboratory of Bone Tissue Engineering, Beijing Laboratory of Biomedical Materials, Beijing Research Institute of Traumatology and Orthopaedics, Beijing Jishuitan Hospital, Beijing 100035, PR China

ARTICLE INFO

Keywords:
Osteosarcoma
Polymersomes
Targeted delivery
Nanomedicine
Adjuvant chemotherapy

ABSTRACT

Osteosarcoma (OS) is a rare but frequently lethal bone malignancy in children and adolescents. The adjuvant chemotherapy with doxorubicin (Dox) and cisplatin remains a mainstream clinical practice though it affords only limited clinical benefits due to low tumor deposition, dose-limiting toxicity and high rate of relapse/metastasis. Here, taking advantage of high IL-11Rα expression in the OS patients, we installed IL-11Rα specific peptide (sequence: cyclic CGRRAGGSC) onto redox-responsive polymersomes encapsulating Dox (IL11-PDox) to boost the specificity and anti-OS efficacy of chemotherapy. Of note, IL-11Rα peptide at a density of 20% greatly augmented the internalization, apoptotic activity, and migration inhibition of Dox in IL-11Rα-overexpressing 143B OS cells. The active targeting effect of IL11-PDox was supported in orthotopic and relapsed 143B OS models, as shown by striking repression of tumor growth and lung metastasis, and substantial survival benefits over free Dox control. We further verified that IL11-PDox could effectively inhibit patient-derived OS xenografts. IL-11Rα-targeted nanodelivery of chemotherapeutics provides a potential therapeutic strategy for advanced osteosarcoma.

1. Introduction

Osteosarcoma (OS) is a most common bone malignancy at the distal femur and proximal tibia in children and adolescents [1]. The surgery combined with adjuvant chemotherapy remains a mainstream clinical practice [2]. Unfortunately, ca. 40–50% patients would encounter tumor relapse and metastasis [3], yielding poor prognosis and a gloomy 5-year survival rate of <30% [4]. The adjuvant chemotherapy mainly adopts doxorubicin (Dox), cisplatin or high-dose methotrexate, which affords only limited clinical benefits due to low tumor deposition and dose-limiting toxicity such as cardiotoxicity and myelosuppression.

Targeted delivery of chemotherapeutics is considered as a promising means to improving chemotherapy of different cancers including OS [5,6]. In the past years, various targeting strategies employing bisphosphonate [7,8], hyaluronic acid [9,10], aptamer [11,12], peptide [13,14] and dual ligands [15,16] have been exploited for OS chemotherapy. The nanovehicles varied from liposomes, nanogels, micelles, to red blood cell membrane coated metal-organic framework [10,17–21]. It should be noted that in spite of considerable work on the development of OS-targeted nanomedicines, most ligands such as bone-affine bisphosphonate, hyaluronic acid, folic acid and cRGD peptide are in fact not specific to OS cells. The insufficient stability and inefficient intracellular drug release of nanomedicines are further problems perplexing their OS-targetability.

IL-11Rα is an OS-associated antigen detected in a majority of advanced OS patients and an indicator for high-risk OS [22,23]. The high IL-11Rα expression is found to correlate with poor prognosis [24]. IL-11Rα-targeted peptidomimetic displayed evident anti-OS therapeutic

* Corresponding author.
** Corresponding authors at: Biomedical Polymers Laboratory, College of Chemistry, Chemical Engineering and Materials Science, and State Key Laboratory of Radiation Medicine and Protection, Soochow University, Suzhou 215123, PR China.
E-mail addresses: chendafujst@126.com (D. Chen), zyzhong@suda.edu.cn (Z. Zhong), fhmeng@suda.edu.cn (F. Meng).
[1] These authors contribute equally to this work.

https://doi.org/10.1016/j.jconrel.2022.08.048
Received 18 July 2022; Received in revised form 22 August 2022; Accepted 23 August 2022
Available online 31 August 2022

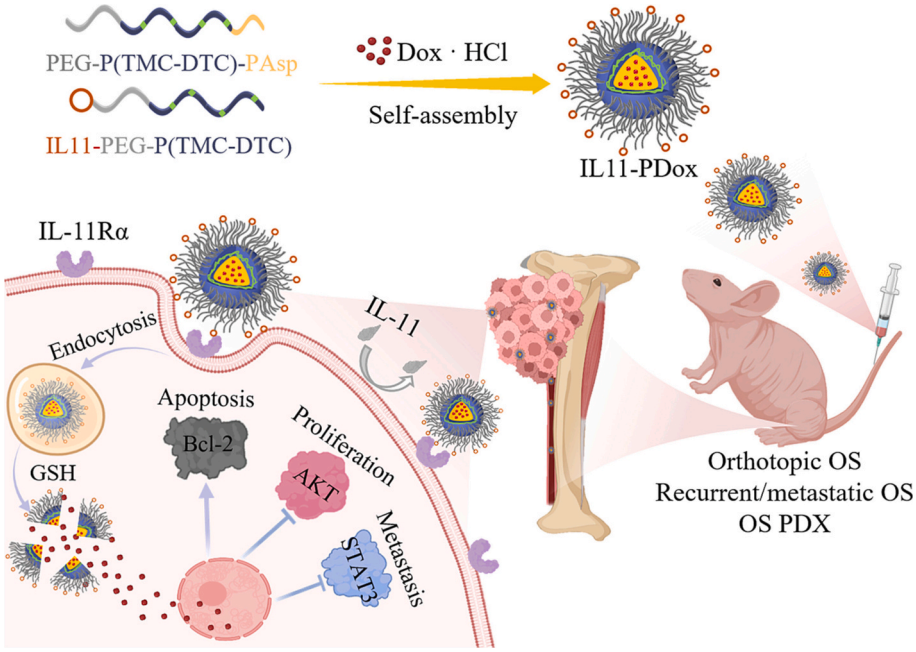

Scheme 1. Illustration of fabricaiton of IL-11Rα-targeting polymersomal Dox (IL11-PDox) and strong inhibition of growth, recurrence and metastasis of malignant osteosarcoma.

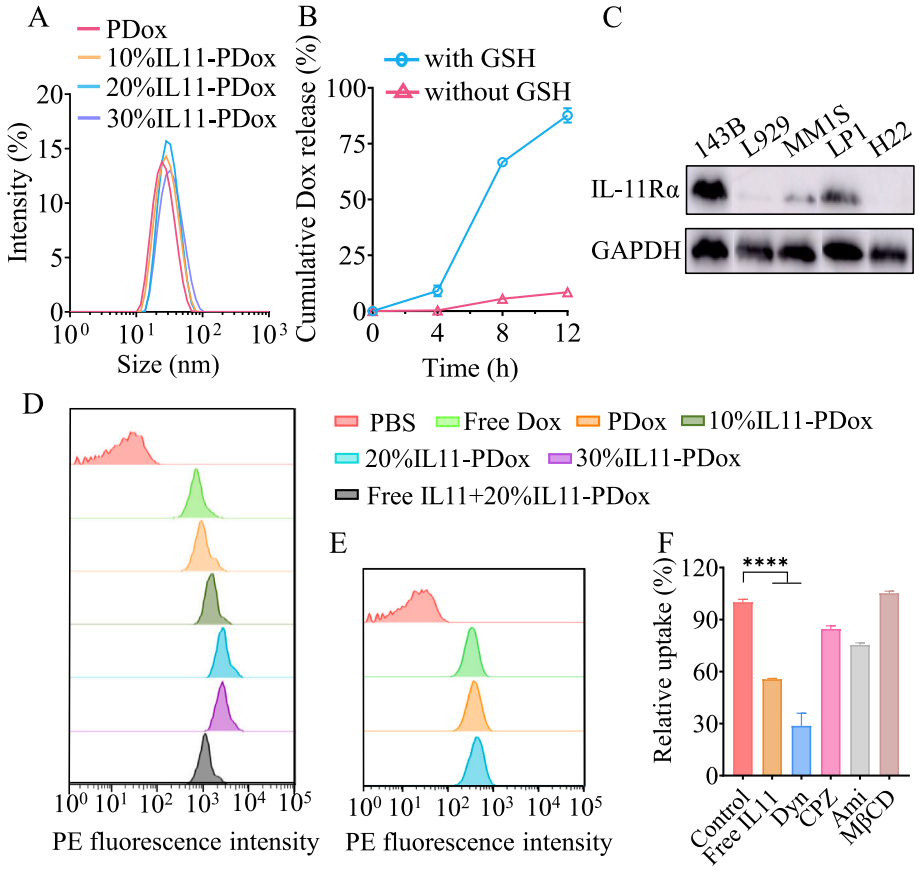

Fig. 1. Characterization of IL11-PDox. (A) Size distribution of IL11-PDox with IL11 peptide contents of 0, 10%, 20% or 30% determined by DLS. (B) In vitro Dox release from IL11-PDox at 37 °C with or without 10 mM GSH (polymersome conc.: 1 mg/mL, $n = 3$). (C) IL-11Rα expression in 143B, L929, MM1S, LP1 and H22 cells determined by western blot. Flow cytometric analyses of 143B (D) or L929 (E) cells following 4 h incubation with free Dox, PDox and IL11-PDox with various contents of IL11 peptide. Free IL11 peptide pretreated 143B cells incubated with 20% IL11-PDox were used as control. (F) Flow cytometry analysis of the endocytosis of Cy5-labeled IL11-P in 143B cells pretreated with free IL11 peptide, Dyn, CPZ, Ami, or MβCD. ****$p < 0.0001$.

efficacy [14]. Interestingly, IL-11 mimic phage showed that short CGRRAGGSC peptide had a high specificity and affinity to IL-11Rα [23,25]. Here, we designed IL-11Rα specific peptide-installed redox-responsive polymersomes encapsulating Dox (IL11-PDox) to boost the specificity and anti-OS efficacy of chemotherapy (Scheme 1). We have previously established that redox-responsive polymersomes based on dithiolane-functionalized poly(trimethylene carbonate) were robust and mediated efficient release of various drugs including Dox, siRNA and

Table 1
Characteristics of PDox and IL11-PDox at Dox theoretical DLC of 4.7 wt%.

Formulation	Size[a] (nm)	PDI[a]	DLC[b] (wt%)	DLE[b] (%)	Zeta[c] (mV)
PDox	25	0.11	4.1	88	−12.7
10%IL11-PDox	27	0.13	4.0	86	−13.0
20%IL11-PDox	29	0.15	4.1	88	−11.4
30%IL11-PDox	33	0.12	4.0	86	−10.1

[a] Determined by DLS.
[b] Determined by UV−vis spectroscopy.
[c] Determined using a Zetasizer Nano-ZS equipped with a capillary electrophoresis cell.

proteins in tumor cells [26–28]. Of note, IL-11 peptide at a density of 20% greatly augmented the specificity and anti-OS efficacy of Dox in IL-11Rα-overexpressing 143B OS cells, orthotopic and relapsed 143B OS models as well as OS patient-derived xenografts (PDX). IL-11Rα-targeted nanodelivery of chemotherapeutics provides a potential therapeutic strategy for advanced osteosarcoma.

2. Experiment

2.1. Preparation and characterization of IL11-PDox

IL11 peptide-functionalized copolymer, IL11-PEG-P(TMC-DTC), was obtained by amidation reaction of IL11 peptide (disulfide cyclic CGRRAGGSC) with NHS-PEG-P(TMC-DTC).

IL11-PEG-P(TMC-DTC) and PEG-P(TMC-DTC)-PAsp both at 40 mg/mL in DMF was mixed at mole ratio of 0/100, 10/90, 20/80, or 30/70. To prepare IL11-PDox, 0.1 mL mixed polymer solution was added to 0.9 mL HEPES buffer (10 mM, pH 7.4) containing Dox·HCl (5 mg/mL, 200 μg for a theoretical loading 4.7 wt%). After stirring at 37 °C for 5 min, IL11-PDox was then dialyzed (MWCO 7000) in HEPES for 8 h (medium changed every 2 h). The size and size distribution were measured by DLS. The Dox content was determined by UV–vis measurement at 480 nm according to the Dox standard curve. To test the stability of IL11-PDox, size changes of polymersomes at 4 °C or 10% FBS were measured at 0, 4, 8 and 14 days or 0, 4, 12 and 24 h.

2.2. Cellular uptake study using flow cytometry

To study the cellular uptake and targetability of IL11-PDox, 143B cells seeded in 6-well plate (1×10^5 /well) were cultured at 37 °C for 24 h, and then 200 μL free Dox, PDox, 10% IL11-PDox, 20% IL11-PDox, 30% IL11-PDox (Dox: 10 μg/mL) and PBS were added. After 4 h, the cells were digested with 500 μL trypsin and collected by centrifugation (1000 ×*g*, 3 min) and PBS washing (×2). Finally, the cells were resuspended in 500 μL PBS, and immediately measured using a BD FACS Calibur flow cytometer to acquire fluorescence histograms (1×10^4 cells) and analyzed using FlowJo-10 software. To investigate whether IL11-PDox entered 143B cells via IL-11Rα, 143B cells were pre-

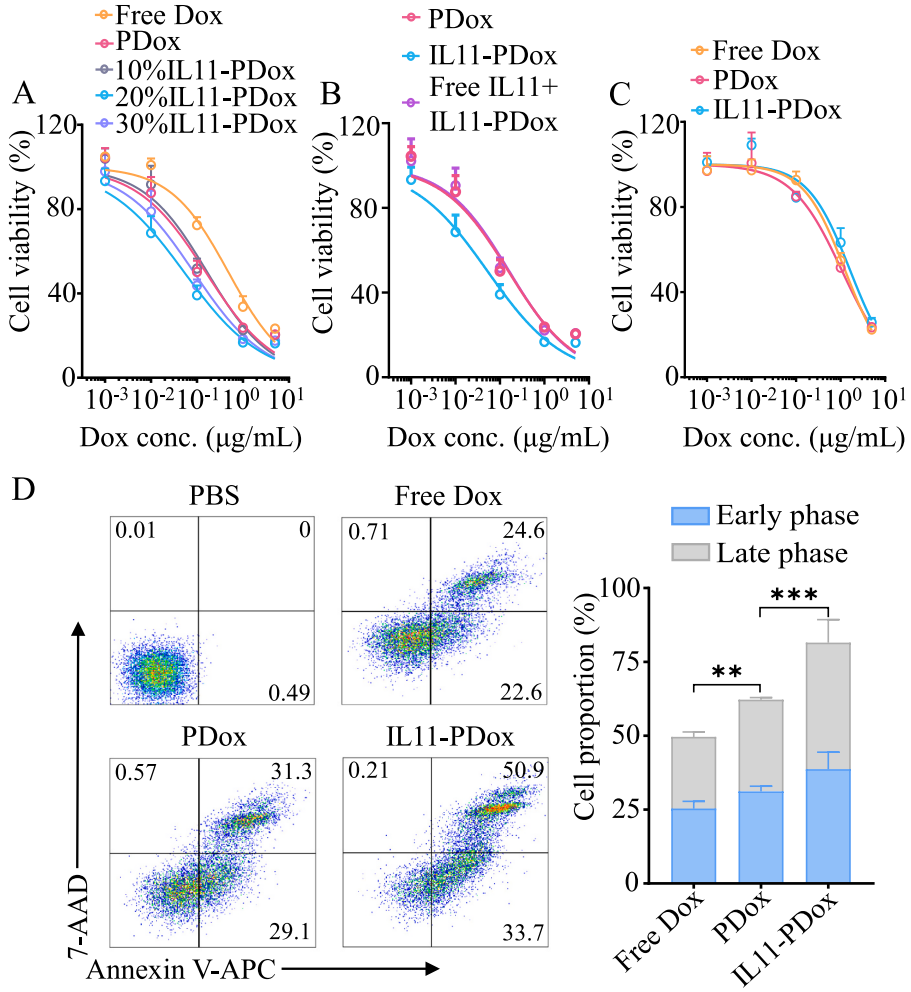

Fig. 2. In vitro anti-tumor activity of IL11-PDox toward 143B cells. (A) MTT assays of 143B cells treated with free Dox and IL11-PDox with IL11 peptide contents of 0, 10%, 20% or 30% ($n = 6$). (B) MTT assays of IL11 peptide-pretreated 143B cells at incubation with 20% IL11-PDox (n = 6). (C) MTT assays of L929 cells treated with free Dox, PDox or IL11-PDox (n = 6). (D) Apoptosis analysis of 143B cells treated with free Dox, PDox and IL11-PDox ($n = 3$). $^{**}p < 0.01$ and $^{***}p < 0.001$.

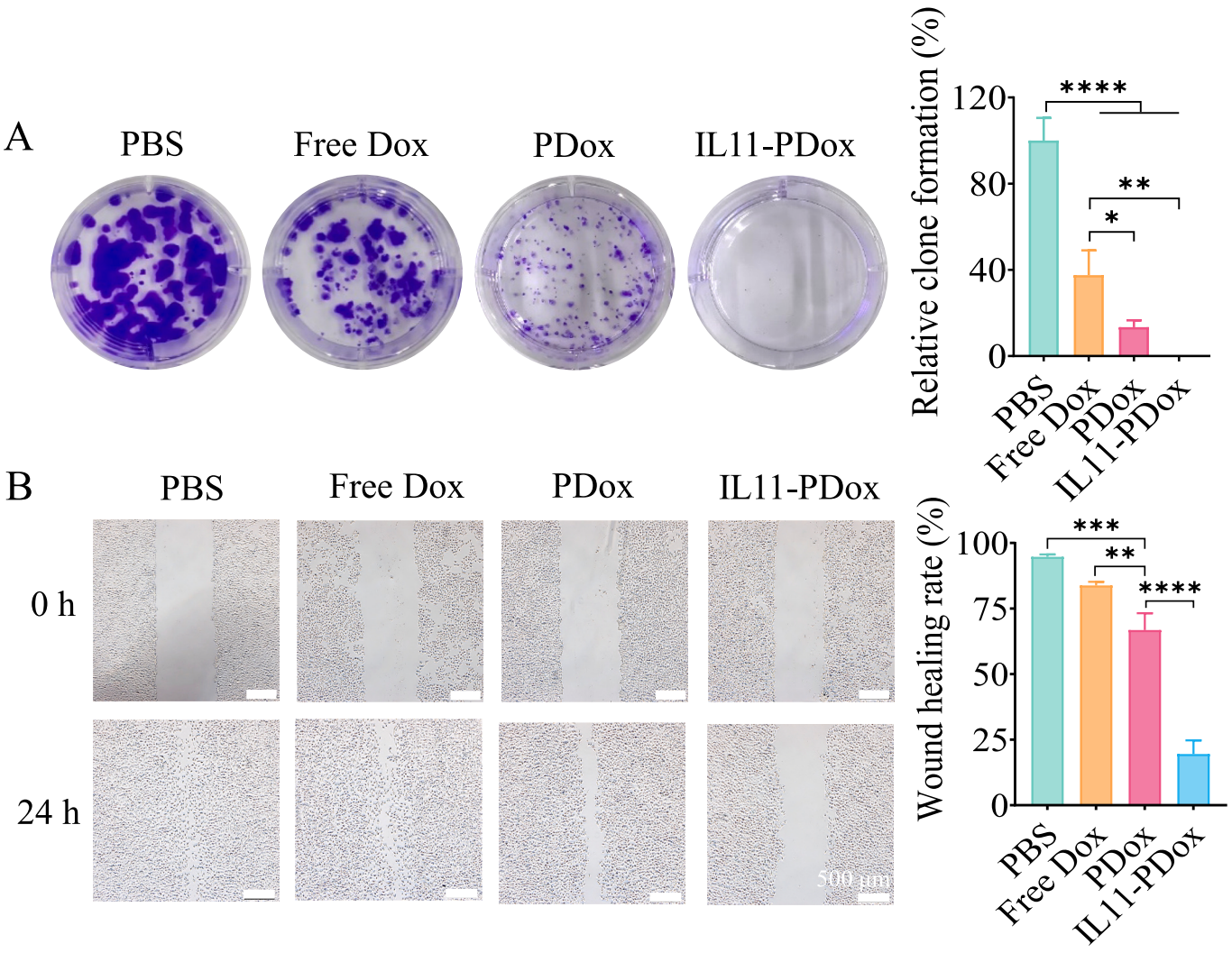

Fig. 3. Clone formation and migration of 143B cells treated with IL11-PDox, PDox or free Dox ($n = 3$). (A) Clone formation and (B) cell migration using scratch-healing assay. *$p < 0.05$, **$p < 0.01$, ***$p < 0.001$ and ****$p < 0.0001$.

incubated with a 20-fold excess of free IL-11 peptide for 2 h before adding IL11-PDox, and then treated the same way as above. In addition, the endocytosis of IL11-PDox by IL-11Rα low-expressing L929 cells was evaluated similarly.

To study the endocytic pathway of the nanomedicine, Cy5-labeled empty polymersomes IL11-P was added to 143B cells pretreated with endocytic pathway inhibitors dynasore (Dyn, 80 μM), chlorpromazine (CPZ, 10 μg/mL), amiloride hydrochloride (Ami, 1 mg/mL), methyl - β -cyclodextrin (MβCD, 1 mg/mL), free IL11 peptide (4 mg/mL), or PBS at 37 °C for 1 h. After 2 h incubation, the cells were treated similarly as above ($n = 3$).

2.3. In vitro cytotoxicity of IL11-PDox

The cytotoxicity of IL11-PDox was evaluated by MTT assays. 143B cells seeded in 96-well plates (2×10^3 /well) were cultured in 5% CO_2 incubator at 37 °C for 24 h, and 20 μL free Dox, PDox, 10% IL11-PDox, 20% IL11-PDox, and 30% IL11-PDox (Dox: 0.001, 0.01, 0.1, 1 and 5 μg/mL) were added. After 4 h, the medium was removed and the cells were incubated with fresh medium for 44 h. Then the cells were treated with 10 μL MTT (5 mg/mL) for 4 h and 150 μL DMSO to dissolve purple formazan crystals. The UV absorbance of cells at 570 nm was measured by multifunctional microplate analyzer. The cell viability (%) was calculated as the percentage of the absorbance of samples of PBS group ($n = 6$). To perform the inhibition experiments, 143B cells were pre-incubated with 20-fold excess of free IL11 peptide for 2 h before adding IL11-PDox, followed by the same procedure. In addition, to investigate the effect of IL11 peptide, the cytotoxicity of IL11-PDox to L929 cells was also evaluated similarly.

To investigate the cytotoxicity of empty polymersomes IL11-P and P to 143B cells and L929 cells, and the cytotoxicity of free IL11 peptide to 143B cells, 20 μL IL11-P and P (polymersome concentration: 0.2, 0.4, 0.8 and 1 mg/mL), and free IL11 peptide (0.5, 1, 1.5, 2, 3 and 4 mg/mL) were incubated with cells at 37 °C for 4 h. The medium was removed and the cells were incubated with fresh medium for 44 h. Then MTT assays were performed similarly ($n = 6$).

2.4. Evaluation of cell apoptosis, cloning formation, and migration of IL11-PDox

143B cells seeded in 6-well plates (1.5×10^5/well) were incubated at 37 °C for 24 h. 200 μL free Dox, PDox, IL11-PDox (Dox: 0.1 μg/mL) and PBS were added. After for 4 h, the cells were then incubated with fresh medium for 44 h. The cells were collected and washed (×2 PBS), and added with Annexin V-APC (5 μL) and 7-AAD (10 μL) to incubate for 5 min at r.t. Apoptosis was measured within 1 h by flow cytometry (early phase channel: APC, late phase channel: 7-AAD) ($n = 3$). Two single staining samples of early or late apoptosis were prepared according to

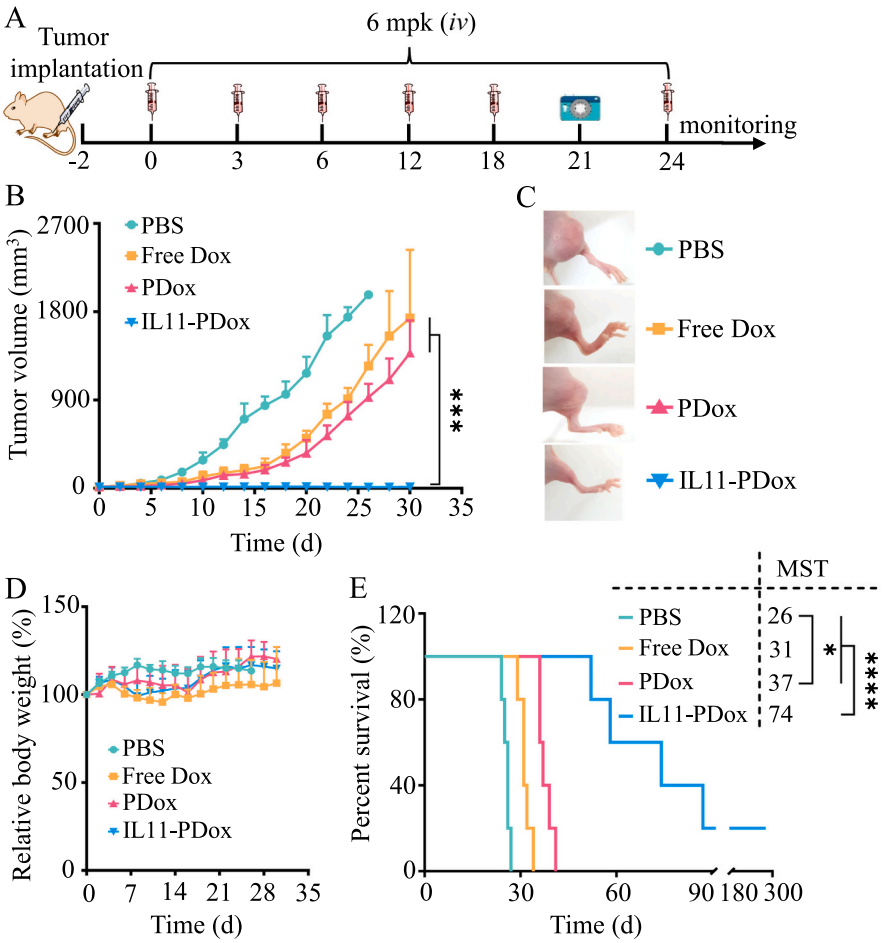

Fig. 4. Therapeutic efficacy of IL11-PDox in 143B orthotopic OS model in nude mice ($n = 5$). (A) Work flow. The mice were treated with free Dox, PDox and IL11-PDox (6 mpk) on day 0, 3, 6, 12, 18 and 24. (B) Tumor growth curves and (C) pictures of mouse hind legs on day 21. (D) Body weight changes and (E) Kaplan–Meier survival curves of mice. $^{*}p < 0.05$, $^{***}p < 0.001$ and $^{****}p < 0.0001$.

the manual.

For clone formation assay, 143B cells seeded in 6-well plates (800 /well) were cultured at 37 °C for 24 h, and added with free Dox, PDox or IL11-PDox (Dox: 0.1 μg/mL). After 4 h, the medium was replaced with drug-free medium for further culture (day 0). In the following 10 days, the medium was refreshed on day 2, 4, 6, and 8. On day 10, the cells were fixed with 4% paraformaldehyde for 20 min and stained with 1% crystal violet for 30 min. After washing, the cells were photographed and semi-quantitatively analyzed with Image J-10 software ($n = 3$).

To study cell migration, 143B cells in 6-well plates (1.5×10^5 /well) were cultured at 37 °C for 24 h, and then incubated with free Dox, PDox and IL11-PDox (Dox: 0.08 μg/mL) for 4 h. Then the confluent cell monolayers were scratched with a 200-μL pipette tip to generate wounds, and fresh medium was added to incubate for 24 h. Images of the wounds at 0 and 24 h were taken using a microscope, and semi-quantitatively analyzed using Image J-10 software to compare the width of scratches to evaluate the cell migration ($n = 3$).

2.5. Establishment of osteosarcoma (OS) tumor models

All animal experiments were approved by the Animal Care and Use Committee of Soochow University and all protocols conformed to the Guide for the Care and Use of Laboratory Animals.

To build orthotopic OS model, 75 μL 143B cells (1×10^6 cells/mouse) containing 30 vol% Matrigel were directly injected into the left tibial membrane of nude mice using syringe (29 gauge). The tumor growth and the conditions of the mice were continuously monitored.

To build recurrent/metastatic OS model, at the tumor volume of the above orthotopic OS of ca. 400 mm^3, the tumor bulks above the muscle were surgically removed in a sterile environment, leaving the tumor at the periosteum to mimic the clinical operation. The wound was sutured and tumor would relapse and metastasize.

To establish a OS patient-derived xenograft (PDX) model, tumor tissue from an OS patient was directly preserved with the patient's informed consent, cut into small pieces (40 mm^3) and directly transplanted subcutaneously into SCID Beige mouse. Tumor growth and the condition of the mice were monitored.

2.6. In vivo antitumor efficacy of IL11-PDox in OS mouse models

To treat orthotopic OS model, two days after inoculation tumor volume reached ca. 50 mm^3, the mice were randomly divided into four groups (the day was designated as day 0). 200 μL PBS, free Dox, PDox or IL11-PDox ($n = 5$) was administrated on day 0, 3, 6, 12, 18, 24 via tail veins at Dox dose of 6 mg/kg (mpk). The tumor volume and body weight of the mice were measured every two days, and the survival rates of the mice were monitored. The mice were considered dead when the mice died or tumor volume exceeded 2000 mm^3. Tumor volume (V) was calculated based on the formula: $V = 0.5 \times (ab^2\text{-}cd^2)$ (mm^3), a and b represent the length and width of the leg at the tumor site (left hind), and c and d represent the length and width of the corresponding part of the right hind leg.

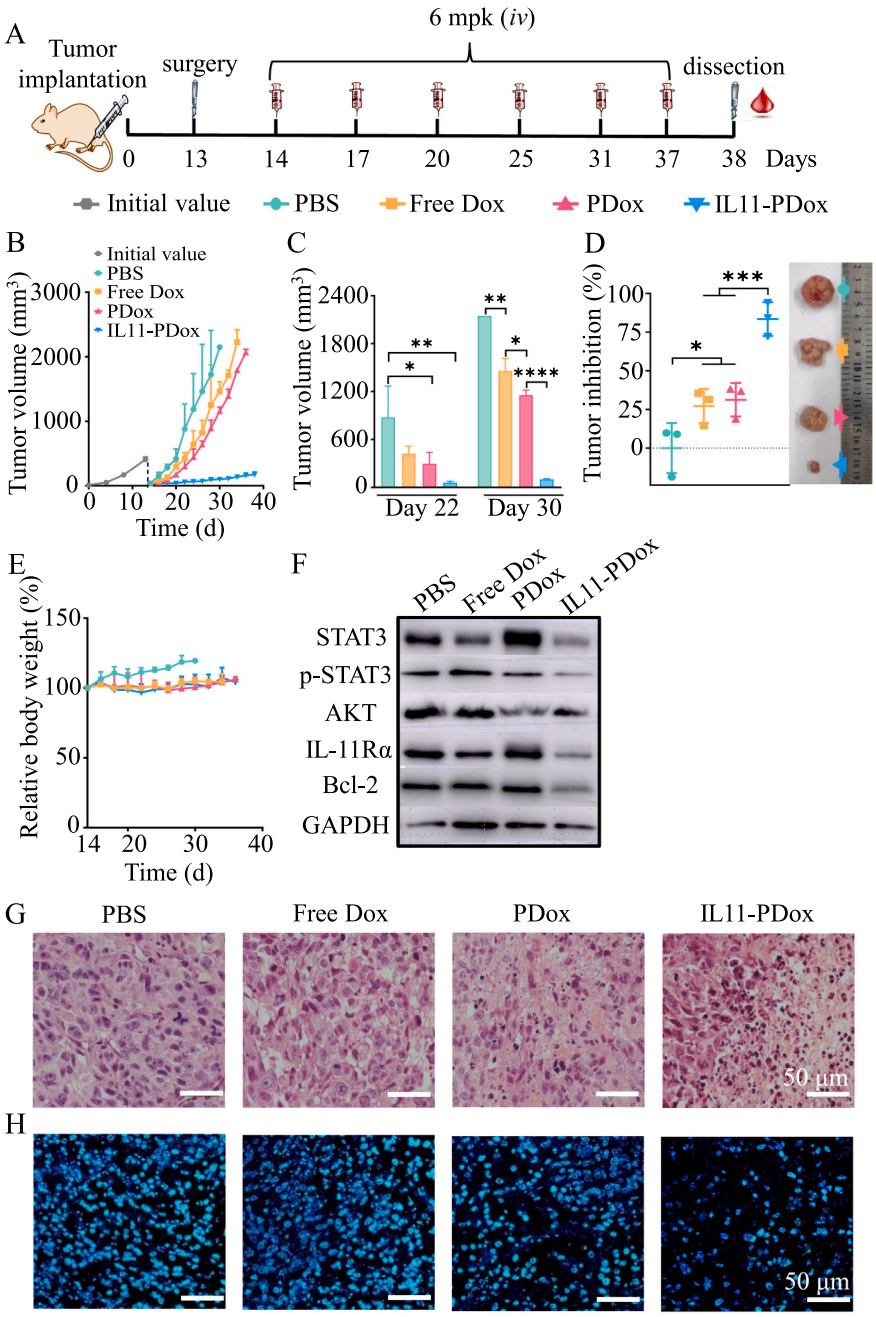

Fig. 5. Therapeutic efficacy of IL11-PDox in post-operative relapsed OS model in nude mice. (A) Work flow. The relapsed OS model was built by surgically removal of the tumor bulks, and treated with IL11-PDox, PDox, free Dox (6 mpk) on day 14, 17, 20, 25, 31, and 37. Tumor growth curves (B) and tumor volume on day 22 and 30 (C) ($n = 3$). (D) Tumor inhibition rate (n = 3) and photograph of isolated tumors. (E) Body weight changes of mice (n = 3). (F) Expression of Bcl-2, IL-11Rα, AKT, STAT3 and p-STAT3 in tumors on day 38. (G) H&E staining images and (H) immunofluorescence of STAT3 staining images in tumor sections on day 38. *$p < 0.05$, **$p < 0.01$, ***$p < 0.001$ and ****$p < 0.0001$.

To treat recurrent/metastatic OS model, on the second day of surgery (day 14), the mice were divided into four groups ($n = 3$) and *iv* injected with 200 μL PBS, free Dox, PDox or IL11-PDox (Dox: 6 mpk) on day 14, 17, 20, 25, 31 and 37. The tumor volume and body weight were measured every two days. On day 38, blood samples were taken for blood routine and biochemical tests. The mice were then sacrificed and dissected to collect heart, liver, spleen, lung, kidney, inguinal lymph nodes and tumors. The tumors and lungs were weighed, photographed and half of tumors were sliced for histological analyses (half for WB). Tumor weight was used to calculate tumor rejection rate (TIR), and lung weight was used to assess lung metastasis. The tumor and main organs were fixed, sliced, stained with H&E for histopathological analysis. Tumor sections were stained with STAT3 antibody immunofluorescence. Whole lung images were scanned and analyzed by Image J-10 to calculate the area percentage of tumor nodules in the total lung tissue. The tumor left was used for determining the expression of apoptosis and metastasis related proteins Bcl-2, IL-11Rα, STAT3, p-STAT3 and AKT using WB.

To treat OS PDX model, at tumor volume of ca. about 50 mm^3, the mice were divided into three groups ($n = 5$) and *iv* injected with 200 μL PBS, free Dox and IL11-PDox (Dox: 4 mpk) on day 0, 5, 12, 19 and 26. The tumor volume and body weight were measured continuously. On day 33, the mice were sacrificed, and the tumors were collected, weighed for TIR calculation, and sliced for H&E histological analysis.

2.7. Statistical analysis

All data are presented as mean ± standard deviation (SD). Statistical difference among groups was assessed by ANOVA analysis of variance. *$p < 0.05$ indicates significant difference, **$p < 0.01$, ***$p < 0.001$ and

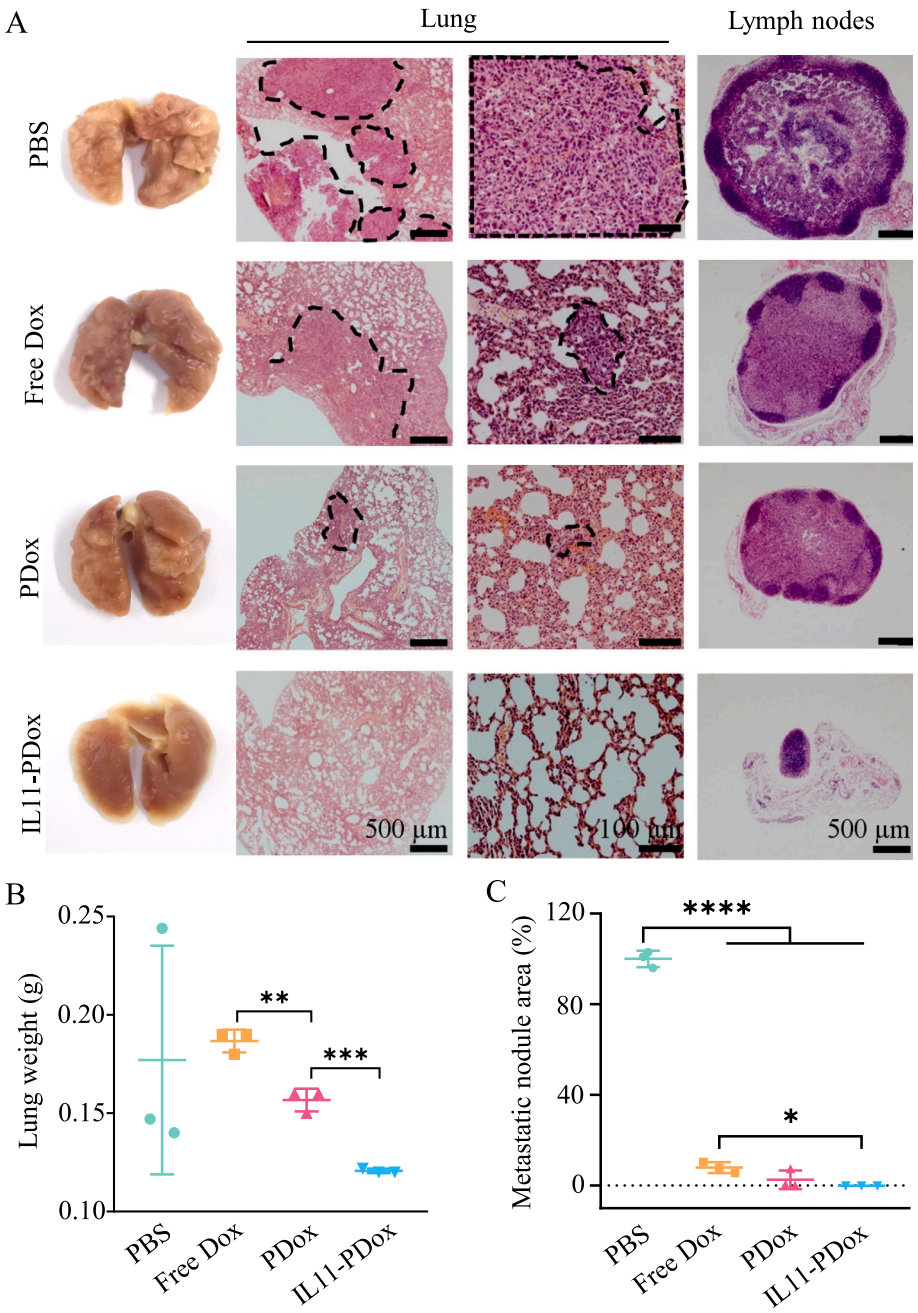

Fig. 6. The inhibition of lung metastasis by IL11-PDox in postoperative relapsed OS model treated as Fig. 5A ($n = 3$). (A) Photographs of isolated lungs and H&E images of slices of lungs and lymph nodes. (B) Lung weight. (C) Metastatic nodules in lung tissues based on area percentage of whole lung scan images. *$p < 0.05$, **$p < 0.01$, ***$p < 0.001$, ****$p < 0.0001$.

****$p < 0.0001$ indicate highly significant difference.

3. Results and discussion

3.1. Preparation and characterization of IL11-PDox

As a first-line drug for OS, Dox has a high potency to kill OS cells. The poor pharmacokinetics, low OS-selectivity and high systemic toxicity, however, seriously limit its clinical efficacy. Liposomal Dox (Doxil) though having improved pharmacokinetics and reduced cardiotoxicity exhibited barely any clinical benefits over free Dox, probably due to lack of tumor-targeting and low tumor deposition. Herewith, we designed IL-11Rα-specific peptide-functionalized disulfide-crosslinked polymersomal Dox (IL11-PDox) for targeted and fast intracellular Dox release to OS cells. Firstly, we measured the IL-11Rα expression in the clinical samples of seven OS patients. The results showed that 6/7 had a high IL-11Rα expression (Fig. S1), confirming that IL-11Rα is an OS-associated antigen [14,22]. Kleinerman et al. reported that IL-11Rα was expressed in 14 of 16 OS patient specimens, and IL-11Rα was seen in the cytoplasm and on cell surface [29].

IL11-PDox was obtained from co-self-assembly of PEG-P(TMC-DTC)-PAsp (5-(15.3–2.3)-1.3 kg/mol) synthesized according to our previous report [27] and IL-11Rα-specific peptide (sequence: cyclic CGRRAGGSC, denoted as IL11)-functionalized PEG-P(TMC-DTC) (IL11-PEG-P(TMC-DTC)) in HEPES buffer (10 mM, pH 7.4) containing Dox·HCl (5 mg/mL). IL11-PEG-P(TMC-DTC) was synthesized by amidation of NHS-PEG-P (TMC-DTC) (7.8–15.3-2.3 kg/mol) [30] with IL11 peptide. Micro BCA assay revealed a peptide functionality of 92.1%. The high IL11 peptide

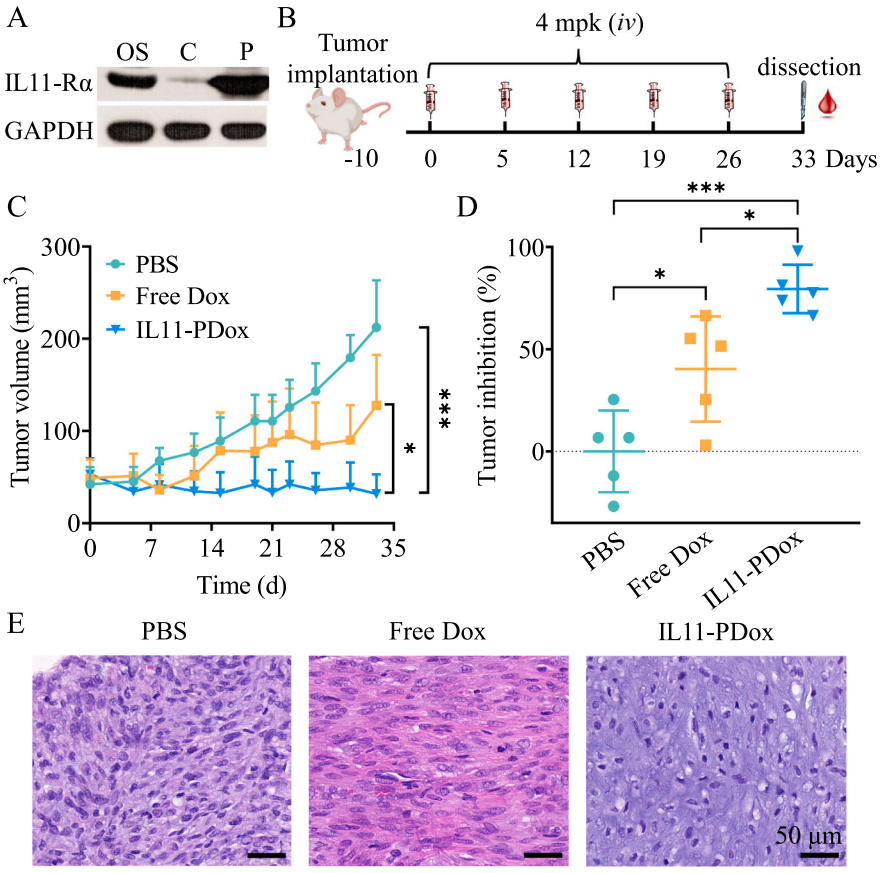

Fig. 7. Therapeutic efficacy of IL11-PDox in OS PDX model (n = 5). (A) Expression of IL-11Rα in patient tumor tissue (OS), normal tissue surrounding the tumor (C) and PDX model (P). (B) Work flow. The mice were treated with IL11-PDox and free Dox (4 mpk) on day 0, 5, 12, 19 and 26. (C) Tumor growth curves. (D) Tumor inhibition rates. (E) H&E staining images of tumor slices. *$p < 0.05$ and ***$p < 0.001$.

functionality was also confirmed by ^{1}H NMR end group analysis (Fig. S2).

IL11-PDox with varying surface IL11 peptide densities from 10%, 20% to 30% was fabricated by adjusting the amount of IL11-PEG-P (TMC-DTC) in the feed. Interestingly, all IL11-PDox had a particularly small size and narrow distribution (Fig. 1A). The size of IL11-PDox increased slightly from 27 to 33 nm with increasing IL11 peptdie densities from 10% to 30% (Table 1). Of note, IL11-PDox was much smaller than the counterparts based on PEG-P(TMC-DTC) (70–80 nm) [31]. We have shown previously that chimaeric polymersomes have generally small sizes [32,33], which could be a potential advantage in tumor penetration [34]. IL11-PDox remained colloidally stable with unchanged size and size distribution after 14-day storage at 4 °C or in 10% FBS solution for 24 h (Fig. S3A—B). Dox leakage from IL11-PDox after 40-day storage was only 1.3%. This high stability of IL11-PDox was owing to spontaneously formed disulfide crosslinks in polymersome membrane as reported previously [27,35]. Notably, ca. 86% Dox was released in 12 h under 10 mM GSH, whereas Dox release was <10% under a non-reductive condition (Fig. 1B). PDox demonstrated similar behavior to IL11-PDox.

3.2. Enhanced endocytosis of IL11-PDox in OS cells

The western blot experiments were conducted to determine the expression of IL-11Rα on different cell lines. The results revealed a very high expression of IL-11Rα in human OS 143B cells while moderate expression in LP1 and MM1S cells, and very low in L929 and H22 cells (Fig. 1C), in accordance to specific expression of IL-11Rα on OS cells [14]. We then investigated the endocytosis of IL11-PDox in 143B cells. The ligand density on nanoparticles plays a vital role in the targetability to tumor cells [36,37]. The flow cytometric results showed that the uptake of IL11-PDox was much higher than that of non-targeting PDox, and IL11-PDox with 20% IL11 peptide gave the highest uptake, which was 2.8- and 3.7-fold that of PDox and free Dox, respectively (Fig. 1D). The uptake of IL11-PDox was greatly reduced in IL11 peptide-pretreated 143B cells (Fig. 1D). While in IL-11Rα-negative L929 cells, the uptake of both IL11-PDox and PDox was low and indistinguishable (Fig. 1E). These results confirmed active targeting effect of IL11-PDox to IL-11Rα-positive OS cells.

CLSM images revealed a fast cell entry of IL11-PDox and even transporting from cytosol to nucleus (nucleolus) quickly from 1 h to 4 h (Fig. S4). Strong Dox fluorescence intensity in nucleolus was observed at 2 h incubation, in great contrast to the low Dox concentration of free Dox and PDox groups, as well as cells pretreated with free IL11 peptide. The results confirmed the flow cytometric results. The prompt endocytosis of IL11-PDox to nuclei or nucleolus of the tumor cells facilitated the binding of DNA to prevent replica and ribosome fabrication, causing cytotoxicity.

To study the endocytic pathway, the uptake of Cy5-labeled IL11-P was investigated in 143B cells pre-treated with dynasore, CPZ, amiloride or MβCD. The results revealed significant inhibition of uptake by dynasore and free IL11 peptide (Fig. 1F), suggesting receptor-mediated and dynamin dependent endocytosis of IL11-P.

3.3. In vitro cytotoxicity and inhibition of cell migration of IL11-PDox

The cytotoxicity studies using MTT assays showed that both PDox and IL11-PDox were significantly more toxic than free Dox to 143B cells

(Fig. 2A). The IC_{50} of 20%IL11-PDox was only 0.05 μg/mL, which was 3.2- and 9.6-fold lower than those of PDox and free Dox, respectively. However, the toxicity of 20%IL11-PDox to IL11 peptide-pretreated 143B cells became similar to PDox (Fig. 2B). To IL-11Rα-negative L929 fibroblasts, 20%IL11-PDox had a similar IC_{50} as PDox and free Dox, and 32-time higher than that to 143B cells (Fig. 2C). The free IL11 peptide and empty polymersomes (P and IL11-P) were non-toxic at 4 mg/mL and 1 mg/mL, respectively (Fig. S3C-E). These results verify the selective killing effect of IL11-PDox to IL-11Rα positive OS cells. IL11-PDox with 20%IL11 was used in subsequent experiments unless otherwise specified.

Fig. 2D shows that IL11-PDox induced 84.6% 143B cells undergoing apoptosis, which was significant compared with free Dox (47.2%) and PDox (60.4%). In particular, IL11-PDox caused more late apoptosis (50.9% versus 24.6% and 31.3% for free Dox and PDox, respectively). The cell cloning results showed that PDox significantly reduced 143B cell clones relative to free Dox, whereas IL11-PDox completely rejected the clone formation (Fig. 3A). The scratch-healing assays displayed fast migration and complete healing of 143B cells in 24 h, in consistent with their high rate of metastasis (Fig. 3B). Interestingly, IL11-PDox markedly inhibited cell migration compared with PDox and free Dox (****p). The above results confirm that IL11-PDox possesses superior selectivity, apoptotic activity, and anti-migration effect toward OS cells.

3.4. Antitumor efficacy of IL11-PDox in 143B orthotopic OS model

To evaluate the anti-OS activity of IL11-PDox in vivo, we established orthotopic OS mouse model by injecting 143B cells into the femoral periosteum of the left hind leg of nude mice using a syringe of 29 gauge. The tumor was highly malignant, rapidly reaching 2000 mm^3 on day 24. The mice exhibited symptoms of mobility difficulties and osteolysis, pointing to successful establishment of orthotopic 143B OS model. To firstly assess the in vivo targetability of IL11-PDox, at tumor volume of ca. 200 mm^3 IL11-PDox, PDox and free Dox were intravenously (*i.v.*) injected into the mice, which were scanned to observe Dox accumulation at tumor sites. Fig. S5A showed that IL11-PDox accumulated at tumor sites quickly after injection, and reached maximum at 4 h, while the tumor enrichment was much lower in both PDox and free Dox groups. The ex vivo images at 24 h illustrated highly enriched IL11-PDox in tumors and low in major organs, in the contrary to PDox and free Dox groups (Fig. S5B). These results reveal the important role of IL11 peptide in promoting IL11-PDox accumulation in 143B tumors.

The therapeutic treatment was started two days after tumor inoculation by *i.v.* injection at a Dox dose of 6 mpk (Fig. 4A-B). Strikingly, IL11-PDox effectively inhibited tumor growth and 3/5 of mice showed no visible tumor in 30 days (Fig. 4B). In contrast, free Dox and PDox only retarded tumor growth and tumors grew rapidly as from day 18 with basically the same growth rate as PBS group. As shown in Fig. 4C, mouse left hind legs on day 21 were paralyzed for PBS group and abnormal for free Dox and PDox groups, in contrast to the healthy legs in IL11-PDox group. It is worth noting that except for free Dox group, the mice treated with both PDox and IL11-PDox did not show body weight loss (Fig. 4D), indicating effective reduction of systemic toxicity. The survival curves disclosed that PDox significantly improved the median survival time (MST = 37 d versus 26 d for PBS group, *p) while the improvement by free Dox was insignificant (Fig. 4E). Remarkably, IL11-PDox prolonged the MST to 74 d, which was highly significant compared with PBS, free Dox and PDox groups (****p). It should further be noted that one mouse was cured by IL11-PDox. These results certify that IL11-PDox can effectively target and inhibit orthotopic 143B tumor in vivo.

3.5. Antitumor efficacy of IL11-PDox in a postoperative relapsed OS model

OS patients after surgery had a recurrence rate of 40%–50%, leading to a low 5-year survival rate of <30% [4]. In order to further explore the efficacy of IL11-PDox for relapsed/metastatic OS, we built relapsed OS model by resecting the tumor bulks surgically on day 13 when orthotopic tumors were about 400 mm^3 (Fig. 5A). It was found that the recurrent tumors grew significantly faster than the primary tumors (Fig. 5B), as also frequently seen in recurrent OS patients. The recurrence and metastasis after surgery was mainly ascribed to residual tumor cells and circulating tumor cells [38,39]. As for primary OS model, free Dox and PDox caused marginal growth retardation of recurrent tumors while IL11-PDox effectively inhibited tumor recurrence and growth (Fig. 5B). The tumor volumes on day 22 and 30 clearly supported a highly significant inhibitory activity of IL11-PDox compared with free Dox and PDox (****p) (Fig. 5C). On day 38, the tumor inhibition rate (TIR) of IL11-PDox was 83.3%, greatly higher than those of free Dox and PDox (***p, Fig. 5D) and the body weight of all treatment groups remained constant (Fig. 5E), indicating that this treatment scheme did not cause significant toxicities.

On day 38, the survived mice were sacrificed and the expression of relevant proteins to apoptosis and metastasis in the tumors were analyzed using western blot. The results showed significantly downregulated expression of IL-11Rα by IL11-PDox, which is in line with selective binding and killing of IL-11Rα-overexpressed tumor cells. The expressions of Bcl-2, AKT, STAT3 and p-STAT3 were considerably lowered in IL11-PDox group (Fig. 5F), supporting a high apoptotic activity, anti-proliferation and anti-metastatic potency of IL11-PDox, respectively. PI3K-AKT pathway is important for cell proliferation and survival [40]. The activation of STAT3 pathway was reported to promote both growth and metastasis of OS cells [41,42]. The H&E staining revealed widespread tumor apoptosis and necrosis by IL11-PDox (Fig. 5G). The STAT3 staining images further showed that IL11-PDox caused a significant decrease in STAT3 expression in tumor (Fig. 5H, Fig. S6).

Lung metastasis is frequently observed in relapsed OS patients [3]. Interestingly, the lung of IL11-PDox group displayed a smooth surface (Fig. 6A) and a mass of ca. 0.12 g (Fig. 6B), which were both similar to that of healthy mouse. In sharp contrast, the lungs of PBS, free Dox and PDox groups exhibited rough surface with abundance of white metastatic nodules and were much heavier than that of IL11-PDox group. The H&E staining images of lung slices confirmed abundant metastatic tumor cells and destruction of alveolar structures in PBS group (Fig. 6A). The lungs of free Dox and PDox groups though retaining an alveolar structure showed obvious tumor nodules. In sharp contrast, no tumor cell infiltration was observed in the lung of IL11-PDox group. The examination of the lung metastases area (Fig. 6C) confirmed the outstanding performance of IL11-PDox in inhibiting lung metastases of relapsed OS model. These results are consistent with significant downregulation of pro-metastatic proteins like STAT3, p-STAT3 and IL-11Rα in tumor tissues (Fig. 5F, Fig. S6) and rejection of cell migration (Fig. 3B). In addition, lymph node enlargement caused by tumor metastasis was observed in all groups except IL11-PDox group (Fig. 6A).

H&E staining of main organs illustrated that in contrast to free Dox, both IL11-PDox and PDox did not cause cardiomyocyte apoptosis (Fig. S7). Further, no obvious histological damage was discerned in liver, spleen and kidney. The blood routine and blood biochemical tests showed that IL11-PDox treatment significantly reduced WBC (*p) and AST (**p) concentrations as compared to PBS, free Dox and PDox (Fig. S8), further confirming the importance of active targeting effect of IL11-PDox in the chemotherapy of OS.

3.6. Antitumor efficacy of IL11-PDox in OS PDX model

Encouraged by its excellent performance in orthotopic primary and relapsed/metastatic OS models, we further investigated the efficacy of IL11-PDox in OS patient-derived xenograft (PDX) model. PDX model is considered more relevant to the development of clinical drugs [43]. The PDX model was established by subcutaneously transplanting OS patient tumor tissue to SCID beige mice. The patient tissue and PDX tumor displayed a high expression of IL-11Rα while low IL-11Rα expression

was detected in the healthy tissue surrounding OS tumor (Fig. 7A), in agreement with the findings from the OS patient specimens, which had low IL-11Rα expression in normal tissues but high in the metastatic tumor nodules [29]. The mice were treated at tumor volume of ca. 50 mm^3 by *i.v.* injection of IL11-PDox at 4 mpk every five days ($n = 5$) (Fig. 7B). The results showed that IL11-PDox completely inhibited tumor growth over 33 days, which was significantly more potent than free Dox (*p) (Fig. 7C). The tumor inhibition rate (TIR) was ca. 80% and 40% for IL11-PDox and free Dox, respectively (Fig. 7D), confirming a greater anti-OS efficacy of IL11-PDox in PDX model. The H&E staining displayed a considerably less dense tumor tissue and more apoptotic cells for IL11-PDox group than for PBS and free Dox groups (Fig. 7E). Moreover, unlike free Dox, IL11-PDox did not cause cardiac toxicity. These results corroborate the active targeting effect of IL11-PDox toward patient-derived OS xenografts. IL-11Rα-targeted nanodelivery empowers chemotherapy for advanced osteosarcoma.

4. Conclusion

We have demonstrated that IL-11Rα specific peptide-installed redox-responsive polymersomes encapsulating Dox (IL11-PDox) greatly empower the specificity and anti-OS efficacy of chemotherapy, which leads to superior inhibition of IL-11Rα-overexpressing 143B orthotopic OS model, tumor recurrence and lung metastasis after surgical resection, and patient-derived xenograft model compared with free Dox. IL11-PDox also displays clearly less toxicity including cardiotoxicity than free Dox. IL11-PDox has unique advantages including small size (~30 nm), high specificity, good stability, redox-responsivity and facile fabrication. IL-11Rα-targeted nanodelivery of Dox offers a highly attractive therapeutic strategy for malignant OS.

Acknowledgements

This work is supported by research grants from the National Natural Science Foundation of China (NSFC 52033006, 52173275, 51973021).

Appendix A. Supplementary data

Supplementary data to this article can be found online at https://doi.org/10.1016/j.jconrel.2022.08.048.

References

[1] J. Gill, R. Gorlick, Advancing therapy for osteosarcoma, Nat. Rev. Clin. Oncol. 18 (2021) 609–624.
[2] A. Luetke, P.A. Meyers, I. Lewis, H. Juergens, Osteosarcoma treatment - where do we stand? A state of the art review, Cancer Treat. Rev. 40 (2014) 523–532.
[3] M.S. Isakoff, S.S. Bielack, P. Meltzer, R. Gorlick, Osteosarcoma: current treatment and a collaborative pathway to success, J. Clin. Oncol. 33 (2015) 3029–U3127.
[4] L.C. Sayles, M.R. Breese, A.L. Koehne, S.G. Leung, A.G. Lee, H.Y. Liu, A. Spillinger, A.T. Shah, B. Tanasa, K. Straessler, F.K. Hazard, S.L. Spunt, N. Marina, G.E. Kim, S. J. Cho, R.S. Avedian, D.G. Mohler, M.O. Kim, S.G. DuBois, D.S. Hawkins, E. A. Sweet-Cordero, Genome-informed targeted therapy for osteosarcoma, Cancer Discov. 9 (2019) 46–63.
[5] S.Y. Wang, H.Z. Hu, X.C. Qing, Z.C. Zhang, Z.W. Shao, Recent advances of drug delivery nanocarriers in osteosarcoma treatment, J. Cancer 11 (2020) 69–82.
[6] D.L. Xie, Z.Q. Wang, J. Li, D.A. Guo, A.P. Lu, C. Liang, Targeted delivery of chemotherapeutic agents for osteosarcoma treatment, Front. Oncol. 12 (2022), 843345.
[7] H. Wu, Y. Luo, D. Xu, X. Ke, T. Ci, Low molecular weight heparin modified bone targeting liposomes for orthotopic osteosarcoma and breast cancer bone metastatic tumors, Int. J. Biol. Macromol. 164 (2020) 2583–2597.
[8] Z. Lei, Z. Mengying, G. Yifei, W. Xiangtao, H. Meihua, Alendronate-modified polydopamine-coated paclitaxel nanoparticles for osteosarcoma-targeted therapy, J. Drug Deliv. Sci. Technol. 53 (2019), 101133.
[9] Y.Y. Chi, X.L. Yin, K.X. Sun, S.S. Feng, J.H. Liu, D.Q. Chen, C.Y. Guo, Z.M. Wu, Redox-sensitive and hyaluronic acid functionalized liposomes for cytoplasmic drug delivery to osteosarcoma in animal models, J. Control. Release 261 (2017) 113–125.
[10] Y. Zhang, F. Wang, M.Q. Li, Z.Q. Yu, R.G. Qi, J.X. Ding, Z.Y. Zhang, X.S. Chen, Self-stabilized hyaluronate nanogel for intracellular codelivery of doxorubicin and cisplatin to osteosarcoma, Adv. Sci. 5 (2018) 1800811.
[11] K. Gui, X. Zhang, F. Chen, Z. Ge, S. Zhang, X. Qi, J. Sun, Z. Yu, Lipid-polymer nanoparticles with CD133 aptamers for targeted delivery of all-trans retinoic acid to osteosarcoma initiating cells, Biomed. Pharmacother. 111 (2019) 751–764.
[12] C. Liang, F. Li, L. Wang, Z.-K. Zhang, C. Wang, B. He, J. Li, Z. Chen, A.B. Shaikh, J. Liu, X. Wu, S. Peng, L. Dang, B. Guo, X. He, D.W.T. Au, C. Lu, H. Zhu, B.-T. Zhang, A. Lu, G. Zhang, Tumor cell-targeted delivery of CRISPR/Cas9 by aptamer-functionalized lipopolymer for therapeutic genome editing of VEGFA in osteosarcoma, Biomaterials 147 (2017) 68–85.
[13] S.Y. Li, T. Zhang, W.G. Xu, J.X. Ding, F. Yin, J. Xu, W. Sun, H.S. Wang, M.X. Sun, Z. D. Cai, Y.Q. Hua, Sarcoma-targeting peptide-decorated polypeptide nanogel intracellularly delivers shikonin for upregulated osteosarcoma necroptosis and diminished pulmonary metastasis, Theranostics 8 (2018) 1361–1375.
[14] V.O. Lewis, E. Devarajan, M. Cardo-Vila, D.G. Thomas, E.S. Kleinerman, S. Marchio, R.L. Sidman, R. Pasqualini, W. Arap, BMTP-11 is active in preclinical models of human osteosarcoma and a candidate targeted drug for clinical translation, Proc. Natl. Acad. Sci. U. S. A. 114 (2017) 8065–8070. Early Ed.
[15] F.Y. Chen, Y.B. Zeng, X.X. Qi, Y.C. Chen, Z. Ge, Z.X. Jiang, X.C. Zhang, Y.M. Dong, H.W. Chen, Z.C. Yu, Targeted salinomycin delivery with EGFR and CD133 aptamers based dual-ligand lipid-polymer nanoparticles to both osteosarcoma cells and cancer stem cells, Nanomedicine 14 (2018) 2115–2127.
[16] S. Feng, Z.-X. Wu, Z. Zhao, J. Liu, K. Sun, C. Guo, H. Wang, Z. Wu, Engineering of bone- and CD44-dual-targeting redox-sensitive liposomes for the treatment of orthotopic osteosarcoma, ACS Appl. Mater. Interfaces 11 (2019) 7357–7368.
[17] W.H. Chen, Q.W. Chen, Q. Chen, C.Y. Cui, S. Duan, Y.Y. Kang, Y. Liu, Y. Liu, W. Muhammad, S.Q. Shao, C.Q. Tang, J.Q. Wang, L. Wang, M.H. Xiong, L.C. Yin, K. Zhang, Z.Z. Zhang, X. Zhen, J. Feng, C.Y. Gao, Z. Gu, C.L. He, J. Ji, X.Q. Jiang, W.G. Liu, Z. Liu, H.S. Peng, Y.Q. Shen, L.Q. Shi, X.M. Sun, H. Wang, J. Wang, H. H. Xiao, F.J. Xu, Z.Y. Zhong, X.Z. Zhang, X.S. Chen, Biomedical polymers: synthesis, properties, and applications, Sci. China Chem. 65 (2022) 1010–1075.
[18] Y. Zhang, L.L. Cai, D. Li, Y.H. Lao, D.Z. Liu, M.Q. Li, J.X. Ding, X.S. Chen, Tumor microenvironment-responsive hyaluronate-calcium carbonate hybrid nanoparticle enables effective chemotherapy for primary and advanced osteosarcomas, Nano Res. 11 (2018) 4806–4822.
[19] E. Gazzane, I. Buondonno, A. Marengo, B. Rolando, K. Chegaev, J. Kopecka, S. Saponara, M. Sorge, C.M. Hattinger, A. Gasco, R. Fruttero, M. Brancaccio, M. Serra, B. Stella, E. Fattal, S. Arpicco, C. Riganti, Hyaluronated liposomes containing H2S-releasing doxorubicin are effective against P-glycoprotein-positive/doxorubicin-resistant osteosarcoma cells and xenografts, Cancer Lett. 456 (2019) 29–39.
[20] S.Y. Li, W.G. Xu, J.X. Ding, Z.D. Cai, Y.Q. Hua, X.S. Chen, Targeted intracellular delivery of shikonin effectively induces osteosarcoma necroptosis with downward lung metastasis, J. Control. Release 259 (2017) E125.
[21] E. Gazzane, I. Buondonno, A. Marengo, B. Rolando, K. Chegaev, J. Kopecka, S. Saponara, M. Sorge, C.M. Hattinger, A. Gasco, R. Fruttero, M. Brancaccio, M. Serra, B. Stella, E. Fattal, S. Arpicco, C. Riganti, Hyaluronated liposomes containing H2S-releasing doxorubicin are effective against P-glycoprotein-positive/doxorubicin-resistant osteosarcoma cells and xenografts, Cancer Lett. 456 (2019) 29–39.
[22] T. Liu, Q. Ma, Y.L. Zhang, S. Ke, K. Yan, X. Chen, Y.H. Wen, Q.Y. Fan, X.C. Qiu, Interleukin-11 receptor alpha is overexpressed in human osteosarcoma, and near-infrared-labeled IL-11R alpha imaging agent could detect osteosarcoma in mouse tumor xenografts, Tumor Biol. 36 (2015) 2369–2375.
[23] V.O. Lewis, M.G. Ozawa, M.T. Deavers, G. Wang, T. Shintani, W. Arap, R. Pasqualini, The interleukin-11 receptor a as a candidate ligand-directed target in osteosarcoma: consistent data from cell lines, orthotopic models, and human tumor samples, Cancer Res. 69 (2009) 1995–1999.
[24] J. Lokau, V. Schoeder, C. Garbers, The role of interleukin-11 in osteosarcoma, Pathologe 41 (2020) 163–167.
[25] V.O. Lewis, IL-11R alpha: a novel target for the treatment of osteosarcoma, in: E. S. Kleinerman (Ed.), Current Advances in Osteosarcoma, 2014, pp. 285–289.
[26] Y. Wei, Y. Sun, J. Wei, X. Qiu, F. Meng, G. Storm, Z. Zhong, Selective transferrin coating as a facile strategy to fabricate BBB-permeable and targeted vesicles for potent RNAi therapy of brain metastatic breast cancer in vivo, J. Control. Release 337 (2021) 521–529.
[27] C. Zhou, Y. Xia, Y. Wei, L. Cheng, J. Wei, B. Guo, F. Meng, S. Cao, J.C.M. van Hest, Z. Zhong, GE11 peptide-installed chimaeric polymersomes tailor-made for high-efficiency EGFR-targeted protein therapy of orthotopic hepatocellular carcinoma, Acta Biomater. 113 (2020) 512–521.
[28] W. Gu, J. An, H. Meng, N. Yu, Y. Zhong, F. Meng, Y. Xu, J. Cornelissen, Z. Zhong, CD44-specific A6 short peptide boosts targetability and anticancer efficacy of polymersomal epirubicin to orthotopic human multiple myeloma, Adv. Mater. 31 (2019), e1904742.
[29] G.X. Huang, L. Yu, L.J.N. Cooper, M. Hollomon, H. Huls, E.S. Kleinerman, Genetically modified T cells targeting interleukin-11 receptor alpha-chain kill human osteosarcoma cells and induce the regression of established osteosarcoma lung metastases, Cancer Res. 72 (2012) 271–281.
[30] Y. Zou, F. Meng, C. Deng, Z. Zhong, Robust, tumor-homing and redox-sensitive polymersomal doxorubicin: a superior alternative to Doxil and Caelyx? J. Control. Release 239 (2016) 149–158.
[31] Y. Wei, X. Gu, Y. Sun, F. Meng, G. Storm, Z. Zhong, Transferrin-binding peptide functionalized polymersomes mediate targeted doxorubicin delivery to colorectal cancer in vivo, J. Control. Release 319 (2020) 407–415.
[32] H. Wang, X. Wang, Y. Zhang, R. Cheng, J. Yuan, Z. Zhong, Systemic delivery of NAC-1 siRNA by neuropilin-targeted polymersomes sensitizes antiangiogenic therapy of metastatic triple-negative breast cancer, Biomacromolecules 21 (2020) 5119–5127.

[33] H. Zheng, B. Guo, X. Qiu, Y. Xia, Y. Qu, L. Cheng, F. Meng, Z. Zhong, Polymersome-mediated cytosolic delivery of cyclic dinucleotide STING agonist enhances tumor immunotherapy, Bioact. Mater. 16 (2022) 1–11.
[34] J. Hu, X. Yuan, F. Wang, H. Gao, X. Liu, W. Zhang, The progress and perspective of strategies to improve tumor penetration of nanomedicines, Chin. Chem. Lett. 32 (2021) 1341–1347.
[35] N. Yu, Y. Zhang, J. Li, W. Gu, S. Yue, B. Li, F. Meng, H. Sun, R. Haag, J. Yuan, Z. Zhong, Daratumumab immunopolymersome-enabled safe and CD38-targeted chemotherapy and depletion of multiple myeloma, Adv. Mater. 33 (2021), e2007787.
[36] P. Mi, H. Cabral, K. Kataoka, Ligand-installed nanocarriers toward precision therapy, Adv. Mater. 32 (2020) 1902604.
[37] A.M. Alkilany, L. Zhu, H. Weller, A. Mews, W.J. Parak, M. Barz, N. Feliu, Ligand density on nanoparticles: a parameter with critical impact on nanomedicine, Adv. Drug Deliv. Rev. 143 (2019) 22–36.
[38] M. Mohme, S. Riethdorf, K. Pantel, Circulating and disseminated tumour cells - mechanisms of immune surveillance and escape, Nat. Rev. Clin. Oncol. 14 (2017) 155–167.
[39] S. Gkountela, F. Castro-Giner, B.M. Szczerba, M. Vetter, J. Landin, R. Scherrer, I. Krol, M.C. Scheidmann, C. Beisel, C.U. Stirnimann, C. Kurzeder, V. Heinzelmann-Schwarz, C. Rochlitz, W.P. Weber, N. Aceto, Circulating tumor cell clustering shapes DNA methylation to enable metastasis seeding, Cell 176 (2019), 98-+.
[40] P. Angulo, G. Kaushik, D. Subramaniam, P. Dandawate, K. Neville, K. Chastain, S. Anant, Natural compounds targeting major cell signaling pathways: a novel paradigm for osteosarcoma therapy, J. Hematol. Oncol. 10 (2017) 10.
[41] Z. Yang, Z. Cai, C. Yang, Z. Luo, X. Bao, ALKBH5 regulates STAT3 activity to affect the proliferation and tumorigenicity of osteosarcoma via an m6A-YTHDF2-dependent manner, EBioMedicine 80 (2022), 104019.
[42] D.Q. Zuo, K.L. Shogren, J. Zang, D.E. Jewison, B.E. Waletzki, A.L. Miller, S. H. Okuno, Z.D. Cai, M.J. Yaszemski, A. Maran, Inhibition of STAT3 blocks protein synthesis and tumor metastasis in osteosarcoma cells, J. Exp. Clin. Cancer Res. 37 (2018) 244.
[43] L. Landuzzi, M.C. Manara, P.-L. Lollini, K. Scotlandi, Patient derived xenografts for genome-driven therapy of osteosarcoma, Cells 10 (2021) 416.